

Structured search algorithm: A quantum leap

Yash Prabhat,^{1,*} Snigdha Thakur,¹ and Ankur Raina²

¹*Department of Physics, Indian Institute of Science Education and Research, Bhopal 462066, India*

²*Department of Electrical Engineering and Computer Science,
Indian Institute of Science Education and Research, Bhopal 462066, India*

(Dated: May 16, 2025)

We introduce a structured quantum search algorithm that leverages entanglement maps and a fixed-point method to minimize oracle query complexity in unsorted datasets. By partitioning qubits into rows based on their entanglement order, the algorithm enables parallel subspace searches, achieving solution identification with at most two oracle calls per row. Experimental results on IBM Kyiv hardware demonstrate successful searches in datasets with up to 5 TB of unsorted data. Our findings indicate that with optimal encoding, the quantum search complexity becomes $\mathcal{O}(1)$, that is, independent of the dataset size N , surpassing both classical $\mathcal{O}(N)$ and Grover's $\mathcal{O}(\sqrt{N})$ scaling. Furthermore, the letter hypothesizes a scalable simulation of the said algorithm using classical means.

Introduction—Quantum computing represents a paradigm shift in computational capabilities, harnessing the principles of quantum mechanics, such as superposition and entanglement, to solve complex problems intractable for classical systems [1–4]. Among the most celebrated demonstrations of quantum advantage is in the solution to the search problem, where the task is to determine whether a specific item S exists within an unsorted dataset \mathcal{D} or not. Classically, such a search requires examining each of the N elements sequentially, resulting in a time complexity of $\mathcal{O}(N)$. Quantum algorithms, most notably Grover's algorithm, leverage quantum interference to achieve a quadratic speedup, reducing the search complexity to $\mathcal{O}(\sqrt{N})$ [5–7]. Despite this breakthrough, the pursuit of even faster quantum search methods remains a central challenge [8–11]. While optimal for unstructured search, Grover's algorithm does not exploit any underlying structure in the data, and its query complexity still scales with the dataset size.

In this letter, we introduce a structured quantum search (SQS) algorithm that fundamentally reimagines the search process by dividing the global search into independent subspace searches over the qubits. By grouping qubits into rows according to their entanglement order and employing a fixed point quantum search (FPQS) method, our algorithm enables parallel subspace searches and achieves solution identification with two oracle queries per row, independent of the dataset size. Experimental demonstrations on IBM quantum hardware validate the approach, successfully searching datasets with up to 5 TB (40 bits \times 2^{40}) of unsorted data in seconds. Our results show that, with optimal encoding, the quantum search complexity becomes $\mathcal{O}(1)$, that is, independent of the dataset size N . This work establishes a new paradigm for quantum search, surpassing both classical $\mathcal{O}(N)$ and existing quantum algorithms' $\mathcal{O}(\sqrt{N})$ scaling, and highlights the critical role of entanglement

structure in unlocking exponential speedups for practical data-intensive tasks.

The structured quantum search (SQS) algorithm can be likened to a treasure hunt using a map. In the classical case, if there are many locations to search, each must be checked individually or by a large team, with the search effort scaling with the number of locations. However, the task would become more efficient if the searchers could act in parallel. Similarly, our algorithm divides the search into independent subspaces of qubits (analogous to map regions). Due to an exponential increase in the search space through quantum parallelism, we only need a logarithmic number of quantum searchers (qubits). If all qubit subspaces are independent and can be searched in parallel, our search time would be constant, independent of the dataset size.

However, the qubits are not always separable; thus, we require a structure based on their entanglement to guide the search through the independent set of qubits. We call this structure the entanglement map, or EM. We generate the EM using information from the encoding and preparation method of the dataset \mathcal{D} . EM contains multiple rows, where each row has a set of qubits that are separable from each other (inter-separable). EM is constituted in a way that the first row contains independent qubits, whereas the second-row qubits depend on the first row, the third on the first two rows, and so on. In other words, EM is a map consisting of labels of qubits in the order of their entanglement. Note that the first row would also contain the qubits that act as control qubits in the controlled operations. The SQS algorithm uses the FPQS algorithm to search the subspace of qubits and the EM to decide the order in which qubits have to be searched. The complexity of the proposed SQS algorithm depends mainly on the number of rows in the EM and remains independent of the size of the dataset N .

In this letter, we use query complexity to benchmark our algorithm [12]. Query complexity is the number of oracle calls required for a successful search. A general oracle denoted by \hat{O} has an associated function $O(x)$ that returns 1 if x is the searched entry else 0. The best classi-

* Contact author; yashp20@iiserb.ac.in

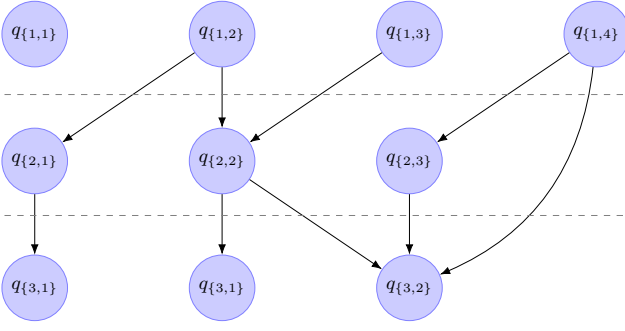


FIG. 1. The schematic figure represents an example of the entanglement order of qubits as encoded in the EM. Each partition corresponds to a row in the EM, and directed edges indicate the entanglement dependencies between qubits in the dataset preparation method. The notation $q_{\{r,c\}}$ represents a qubit at row r and index c of the EM.

cal ordered search, the binary search algorithm, requires $\mathcal{O}(\log N)$ oracle calls to search an item S in a sorted dataset \mathcal{D} [13, 14]. The SQS algorithm incorporates the FPQS algorithm to search through any number of inter-separable qubits in two oracle calls. In our approach, a dataset is adeptly mapped to n qubits such that $n - 1$ qubits are inter-separable and are entangled only to the last qubit n . This encoding with the EM having only two rows allows us to search through a dataset in a maximum of four oracle calls, resulting in a $\mathcal{O}(1)$ complexity.

We encode the dataset \mathcal{D} into the state $|\psi\rangle$ using n data qubits by basis encoding [2, 15, 16]. In Appendix A, we present a novel method to encode a dataset \mathcal{D} for an efficient EM. We denote solution state $|S\rangle$, indicative of the item S in the dataset \mathcal{D} . All other superposition states are denoted by $|R\rangle$, representing the non-solution states. Therefore, any state $|\psi\rangle$ of n qubits is given by

$$|\psi\rangle = \cos\theta |R\rangle + \sin\theta |S\rangle, \quad (1)$$

where $|S\rangle$ and $|R\rangle$ are normalized and are orthogonal to each other,

$$\langle S|S\rangle = 1, \quad \langle R|R\rangle = 1, \quad \langle S|R\rangle = 0, \quad (2)$$

where $\sin\theta = \langle S|\psi\rangle$ and $\cos\theta = \langle R|\psi\rangle$ are the amplitudes of $|S\rangle$ and $|R\rangle$ respectively. Mathematically, the crux of the problem is whether the state $|\psi\rangle$ contains the solution state $|S\rangle$ with a non-zero probability ($\sin^2\theta > 0$) or not. The SQS algorithm drastically reduces the search space by individually searching the subspace of each qubit in the order of their entanglement using the EM. It splits the search into each qubit's subspace and then searches the qubits in the order of their entanglement. The labelling of qubits in the order of their entanglement through EM can be seen as a directed graph, a schematic representation of which is given by Fig. 1. Here, each partition corresponds to a row in the EM, and directed edges indicate the entanglement dependencies between qubits in the dataset preparation method.

Fixed point quantum search—To individually search the subspace of each qubit, we propose the fixed point method. The method fixes a point of convergence, where the search is deemed to be complete [17–23]. We use q_m to denote a separable qubit, while the entangled qubits are discussed later along with EM. The method requires q_m to have an associated ancilla qubit a_m , which acts as a point of convergence for the subspace of q_m . To search the subspace of the qubit q_m , we must first prepare it in its respective preparation state $|\psi_m\rangle$. Where $|\psi_m\rangle$ must reflect the structural encoding of the dataset \mathcal{D} for the subspace of qubit q_m . We define a state preparation operator $\hat{P}(\theta_m)$,

$$\hat{P}(\theta_m) = \hat{R}_Y(\theta_m) = \begin{bmatrix} \cos\theta_m & -\sin\theta_m \\ \sin\theta_m & \cos\theta_m \end{bmatrix}, \quad (3)$$

for q_m as a Pauli Y rotation operator $\hat{R}_Y(\theta_m)$. The parameterization angle θ_m is determined by the binary patterns in the data entries in \mathcal{D} . We refer the reader to Appendix A for the method used to prepare the dataset. The action of $\hat{P}(\theta_m)$ on the quantum state of interest gives us the preparation state $|\psi_m\rangle$ as

$$|\psi_m\rangle = \hat{P}(\theta_m) |0\rangle = \cos\theta_m |R_m\rangle + \sin\theta_m |S_m\rangle, \quad (4)$$

where $|S_m\rangle$ and $|R_m\rangle$ are, respectively, the orthogonal solution and non-solution states for the subspace of q_m . In the case of all n separable qubits, $|S_m\rangle$ is related to $|S\rangle$ as

$$|S\rangle = \bigotimes_{m=1}^n |S_m\rangle. \quad (5)$$

In this work, generating a dataset for search purposes using quantum methods requires the state $|\psi_m\rangle$ in Eq. (4) to be

$$|\psi_m\rangle \in \left\{ |R_m\rangle, |S_m\rangle, \frac{|R_m\rangle + |S_m\rangle}{\sqrt{2}} \right\}. \quad (6)$$

This is achieved by θ_m :

$$\theta_m \in \left\{ 0, \frac{\pi}{2}, \frac{\pi}{4} \right\} \quad (7)$$

for all separable qubits q_m . Entanglement is required for the datasets of size $N \neq 2^n$ and is discussed later.

We present the fixed point operator that flips the ancilla qubit to state $|1\rangle$ to denote convergence. All the ancilla qubits are initialised in state $|0\rangle$. From Eq. (4) the combined initial state $|\Psi_m\rangle$ of a separable qubit q_m and its associated ancilla a_m is

$$|\Psi_m\rangle = |0_{a_m}\rangle |\psi_m\rangle = |0_{a_m}\rangle (\cos\theta_m |R_m\rangle + \sin\theta_m |S_m\rangle). \quad (8)$$

A fixed point operator $\hat{F}_m(\gamma)$, where γ is an arbitrary angle, acting on the m^{th} ancilla a_m and data qubit q_m is defined in the orthogonal basis

$$\{|0_{a_m}\rangle |R_m\rangle, |0_{a_m}\rangle |S_m\rangle, |1_{a_m}\rangle |R_m\rangle, |1_{a_m}\rangle |S_m\rangle\}. \quad (9)$$

Its action on the state $|\Psi_m\rangle$ gives us

$$\hat{F}_m(\gamma)|\Psi_m\rangle = \begin{bmatrix} -\cos(2\gamma) & 0 & 0 & -\sin(2\gamma) \\ -\sin(2\gamma) & 0 & 0 & \cos(2\gamma) \\ 0 & 0 & 1 & 0 \\ 0 & 1 & 0 & 0 \end{bmatrix} \begin{bmatrix} \cos\theta_m \\ \sin\theta_m \\ 0 \\ 0 \end{bmatrix}, \quad (10)$$

where $\hat{F}_m(\gamma)$ marks the ancilla qubit a_m for the state $|S_m\rangle$. The action of $\hat{F}_m(\theta_m)$ on $|\Psi_m\rangle$ is

$$\hat{F}_m(\theta_m)|\Psi_m\rangle = -\cos\theta_m|0_{a_m}\rangle(\cos 2\theta_m|R_m\rangle + \sin 2\theta_m|S_m\rangle) + \sin\theta_m|1_{a_m}\rangle|S_m\rangle, \quad (11)$$

here $\hat{F}_m(\theta_m)$ couples the subspace solution state $|S_m\rangle$ of q_m to the state $|1_{a_m}\rangle$ of the ancilla a_m . This preserves the solution state's amplitude $\sin\theta_m$ from Eq. (8). Then, we measure the m^{th} ancilla qubit a_m to check for convergence. If the state $|1_{a_m}\rangle$ is obtained (probability $\sin^2\theta_m$), we declare convergence to the subspace solution state $|S_m\rangle$ for qubit q_m . If the state $|0_{a_m}\rangle$ is obtained (probability $\cos^2\theta_m$), we get the state

$$|\Psi'\rangle_m = |0_{a_m}\rangle(\cos(2\theta_m)|R_m\rangle + \sin(2\theta_m)|S_m\rangle), \quad (12)$$

where $|\Psi'\rangle_m$ is the combined state of q_m and a_m after measurement collapses a_m to the state $|0_{a_m}\rangle$. Comparing Eq. (12) with the initial state from Eq. (8), the information of the rotation angle θ_m is preserved as $2\theta_m$. This allows convergence to the state $|S_m\rangle$ after multiple measurements on ancilla a_m . We apply $\hat{F}_m(\theta_m)$ a second time, giving us:

$$\hat{F}_m(\theta_m)|\Psi'\rangle_m = -\cos(2\theta_m)|0_{a_m}\rangle(\cos(2\theta_m)|R_m\rangle + \sin(2\theta_m)|S_m\rangle) + \sin(2\theta_m)|1_{a_m}\rangle|S_m\rangle, \quad (13)$$

to obtain $|1_{a_m}\rangle$ with probability $\sin^2(2\theta_m)$. From Eq. (11 and 13), single and double operations of $\hat{F}_m(\theta_m)$ would give convergence probabilities of $\sin^2\theta_m$ and, $\sin^2(2\theta_m)$ respectively. From Eq. (7), the three values of θ_m form three cases with required operations for convergence as

$$\theta_m = \begin{cases} \frac{\pi}{2} & \text{convergence after one operation of } \hat{F}_m(\frac{\pi}{2}); \\ \frac{\pi}{4} & \text{convergence after two operations of } \hat{F}_m(\frac{\pi}{4}); \\ 0 & \text{solution state } |S_m\rangle \text{ does not exist.} \end{cases}$$

Thus, if the subspace solution state $|S_m\rangle$ exists, we converge to it in a maximum of two calls to operator \hat{F}_m . Since \hat{F}_m is a two-qubit operator and does not affect other qubits, it can be applied simultaneously on any number of separable qubits in a single oracle call. We refer the reader to Appendix B for respective calculations and quantum circuits incorporating the oracle in the fixed point operator. We use this method to search each row in the EM before moving to the next row. This allows us to converge all inter-separable qubits to their respective solution states in two oracle calls. When an entry is to be searched in an equal superposition starting state, it can be done in a maximum of two oracle calls, independent of the dataset size N .

Structured quantum search— The $\hat{F}_m(\theta_m)$ operator allows the FPQS algorithm to search any number of inter-separable qubits at once. The question arises: which qubits are inter-separable, and when can they be searched? To solve this, the SQS algorithm uses the entanglement order of qubits in the form of the EM as a guide for the search. EM of n data qubits refers to relabeling the qubits into a two-dimensional map with rows representing the entanglement order of the qubits. Row r , $r \in \{1, \dots, l\}$ in the EM, contains n_r inter-separable qubits, denoted by Q_r :

$$Q_r = \{q_{\{r,1\}}, q_{\{r,2\}}, \dots, q_{\{r,n_r\}}\}, \quad (14)$$

having cardinality $|Q_r| = n_r$. Fig. 1 represents a directed graph of the entanglement order of qubits using this notation. The respective subspace solution state $|S_{Q_r}\rangle$ for row r is given by:

$$|S_{Q_r}\rangle = \bigotimes_{c=1}^{n_r} |S_{\{r,c\}}\rangle, \quad (15)$$

where, $|S_{\{r,c\}}\rangle$ represents the solution state of a data qubit $q_{\{r,c\}}$. Rest of the non-solution states in the subspace of Q_r are given as $|R_{Q_r}\rangle$ satisfying

$$\langle R_{Q_r} | S_{Q_r} \rangle = 0. \quad (16)$$

The qubits in Q_{r+1} are entangled with the qubits in the previous rows, described with the super-set Q_r :

$$Q_r = \{Q_1, Q_2, \dots, Q_r\}. \quad (17)$$

The operations used for entanglement are defined later in Eq. (21); these do not affect the state of already searched qubits. The algorithm searches row by row, where rows are arranged in the order of entanglement of the qubits. The subspace solution state of qubits in Q_r is denoted as $|S_{Q_r}\rangle$:

$$|S_{Q_r}\rangle = \bigotimes_{j=1}^r |S_{Q_j}\rangle, r \in \{1, \dots, l\}. \quad (18)$$

Rest of the non-solution states in the subspace of Q_r are given as $|R_{Q_r}\rangle$ satisfying:

$$\langle S_{Q_r} | R_{Q_r} \rangle = 0. \quad (19)$$

We note that $|S_{Q_r}\rangle$ and $|R_{Q_r}\rangle$ span the whole subspace of the qubits in Q_r . The qubits in Q_{r+1} are prepared and searched using the qubits in Q_r after they have converged to their respective subspace solution state $|S_{Q_r}\rangle$. This discards preparation of the states $|R_{Q_r}\rangle$ containing any non-solution state $|R_{\{j,c\}}\rangle$, $j \in \{1, \dots, r\}$ and $c \in \{1, \dots, n_j\}$. Therefore, the search space is drastically reduced, and the search is fast-tracked. We can represent this search space reduction as a binary tree, shown in Fig. 2. With this convention, Q_l represents all

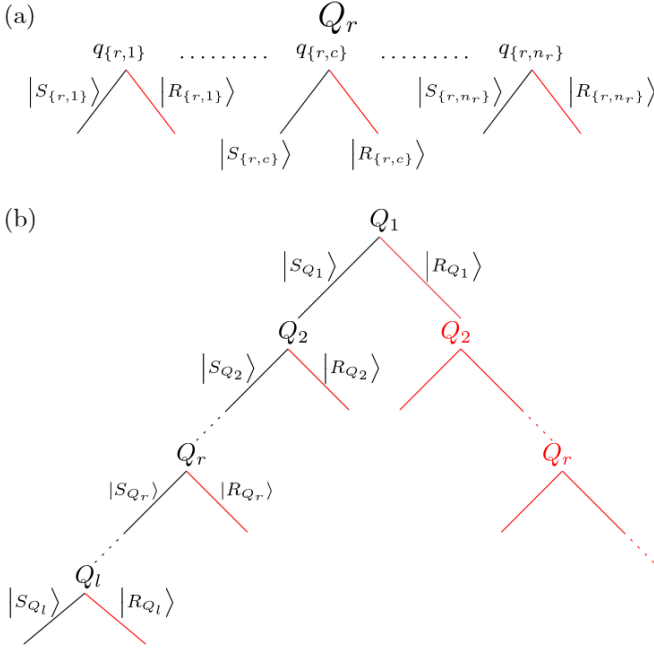


FIG. 2. Binary tree representation for searching n data qubits using EM. (a) represents the parallel search for qubits in Q_r . (b) represents the row-by-row search. The qubits in Q_{r+1} are prepared using the information of the state $|S_{Q_r}\rangle$ in Q_r qubits. The search space in red is discarded by the measurement of the state $|\mathcal{R}_{Q_r}\rangle$.

the data qubits, and the solution state $|S\rangle$ is represented as $|S_{Q_l}\rangle$ by combining all the subspace solution states:

$$|S\rangle = |S_{Q_l}\rangle = \bigotimes_{r=1}^l |S_{Q_r}\rangle. \quad (20)$$

We note that the EM and $|S\rangle$ may not have the qubits in the same sequence. Thus, the above equation may require a rearrangement of qubits.

The algorithm can simultaneously search all the separable qubits, attaining the best performance. Thus, during dataset preparation, it is necessary to keep the number of non-separable qubits to a minimum. We also need to ensure that while entangling the qubits in a row r , we preserve the subspace solution state $|S_{Q_{r-1}}\rangle$ that has been searched for in the qubits Q_{r-1} . For this purpose we use a unitary operator $\hat{A}_{\{r,c\}}$ to entangle the qubits in Q_{r-1} with a qubit $q_{\{r,c\}}$ at an index c , $c \in \{1, \dots, n_r\}$ in row r :

$$\begin{aligned} \hat{A}_{\{r,c\}} = & |S_{Q_{r-1}}\rangle \langle S_{Q_{r-1}}| \otimes \hat{R}_Y(\alpha_{\{r,c\}}) \\ & + \sum_{x \in \mathcal{R}_{Q_{r-1}}} |x\rangle \langle x| \otimes \hat{R}_Y(\beta_{\{r,c\}}^x), \end{aligned} \quad (21)$$

where $\mathcal{R}_{Q_{r-1}}$ represents the set of non-solution states that make up the state $|\mathcal{R}_{Q_{r-1}}\rangle$ in the subspace of Q_{r-1} :

$$|\mathcal{R}_{Q_{r-1}}\rangle = \sum_{x \in \mathcal{R}_{Q_{r-1}}} a_x |x\rangle, \quad (22)$$

where a_x represents the amplitude of the non-solution state $|x\rangle$. Additionally, the rotation operation \hat{R}_Y is the Pauli Y rotation defined in Eq. (3) parameterized by the angles $\alpha_{\{r,c\}}$ and $\beta_{\{r,c\}}^x$ required for the preparation of the qubit $q_{\{r,c\}}$. Here, $\hat{A}_{\{r,c\}}$ acts on the subspace of $(|Q_{r-1}| + 1)$ qubits, where $|Q_{r-1}|$ is given as:

$$|Q_{r-1}| = \sum_{j=1}^{r-1} |Q_j| = \sum_{j=1}^{r-1} n_j, \quad (23)$$

where n_j is the number of qubits in the j^{th} row. The combination of $\hat{A}_{\{r,c\}}$ and $\hat{R}_Y(\theta_{\{r,c\}})$ operators, with $\theta_{\{r,c\}}$ being the single-qubit rotation angle of the qubit $q_{\{r,c\}}$, gives the state preparation operator $\hat{M}_{\{r,c\}}$:

$$\hat{M}_{\{r,c\}} = \hat{A}_{\{r,c\}} \cdot \left(I^{\otimes |Q_{r-1}|} \otimes \hat{R}_Y(\theta_{\{r,c\}}) \right), \quad (24)$$

where I is a single-qubit identity gate. $\hat{M}_{\{r,c\}}$ entangles and prepares the qubit $q_{\{r,c\}}$ after all the qubits in Q_{r-1} converge to their respective solution states $|S_{Q_{r-1}}\rangle$. The subspace solution state $|S_{Q_{r-1}}\rangle$ of the previously searched qubits in Q_{r-1} is preserved by Eq. (21). The action of $\hat{M}_{\{r,c\}}$ on the qubit $q_{\{r,c\}}$ with qubits in Q_{r-1} as control qubits is

$$\hat{M}_{\{r,c\}} |S_{Q_{r-1}}\rangle |0_{\{r,c\}}\rangle = |S_{Q_{r-1}}\rangle |\phi_{\{r,c\}}\rangle, \quad (25)$$

where $|\phi_{\{r,c\}}\rangle$ is the modified starting state of qubit $q_{\{r,c\}}$. Here, the states $|\mathcal{R}_{Q_{r-1}}\rangle |\phi_{\{r,c\}}\rangle$ where the solution cannot be found are discarded, and the subspace solution state $|S_{Q_{r-1}}\rangle$ of the previous rows is preserved. We always converge to the state $|S_{Q_{r-1}}\rangle$ in qubits Q_{r-1} before we prepare the qubits in the row r . Thus, the operator $\hat{M}_{\{r,c\}}$ is equivalent to a combination of single-qubit \hat{R}_Y rotation operators. \hat{R}_Y is additive in angle, and thus, similar to Eq. (3), $\hat{M}_{\{r,c\}}$ can further be written as the preparation operator $\hat{P}(\gamma_{\{r,c\}})$,

$$\hat{P}(\gamma_{\{r,c\}}) = \hat{R}_Y(\theta_{\{r,c\}} + \alpha_{\{r,c\}}), \quad (26)$$

where $\gamma_{\{r,c\}}$,

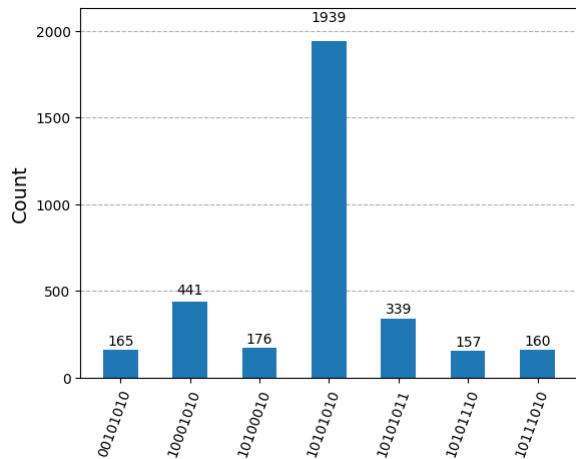
$$\gamma_{\{r,c\}} = \theta_{\{r,c\}} + \alpha_{\{r,c\}}, \quad (27)$$

is the total rotation angle. The action of $\hat{P}(\gamma_{\{r,c\}})$ on the state $|0_{\{r,c\}}\rangle$ gives the state $|\phi_{\{r,c\}}\rangle$ as

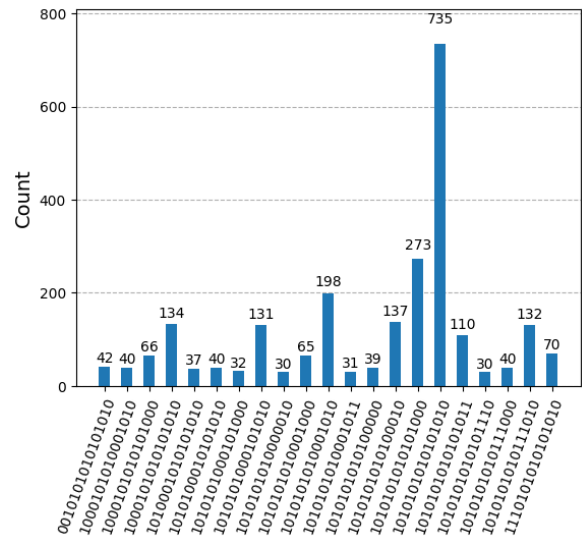
$$\hat{P}(\gamma_{\{r,c\}}) |0_{\{r,c\}}\rangle = |\phi_{\{r,c\}}\rangle. \quad (28)$$

Similar to Eq. (6 and 7), the optimized preparation of $q_{\{r,c\}}$ has the rotation angle $\gamma_{\{r,c\}} \in \{0, \pi/4, \pi/2\}$. The net state preparation operator $\hat{P}(\gamma_{\{r,c\}})$ of a qubit $q_{\{r,c\}}$ is equivalent to a single-qubit operation allowing us to search entangled qubits using the fixed point method discussed earlier.

We prepare and search qubits row by row in the order of the EM, using the FPQS algorithm to mark the



(a) The figure shows the search results for the bit string ‘01010101’ in a dataset of 2^8 bit strings.



(b) The figure shows the search results for the bit string ‘0101010101010101’ in a dataset of 2^{16} bit strings.

FIG. 3. The quantum computer IBM Kyiv used 16 (8 data + 8 ancilla qubits) and 32 (16 data + 16 ancilla) qubits to search through 2^8 and 2^{16} states in equal superposition. (a) shows the search for the bit string ‘01010101’ (‘01’ \times 4), resulting in 1939 counts, and (b) shows the search for the bit string ‘0101010101010101’ (‘01’ \times 8), resulting in 735 counts in 4096 shots. Here, we see multiple states due to hardware noise, of which the lower counts have been removed for clarity.

respective ancilla qubit $a_{\{r,c\}}$ to state $|1\rangle$ if $q_{\{r,c\}}$ converges to $|S_{\{r,c\}}\rangle$. Measurement of all the ancilla qubits in state $|1\rangle$ denotes the existence of the searched entry in the dataset. If $a_{\{r,c\}}$ is found in state $|0\rangle$ for any $\{r,c\}$ in the EM, the solution state $|S\rangle$ does not exist and the search is terminated. Using $\hat{F}(\gamma_{\{r,c\}})$ and $\hat{P}(\gamma_{\{r,c\}})$ from Eq. (10 and 26), we can simultaneously search for the subspace solution state $|S_{Q_r}\rangle$ in all inter-separable qubits Q_r in row r , in two oracle calls. Thus, the search speed would benefit from encoding the dataset so that the EM has the minimum number of possible rows. We refer the reader to Appendix B3 for the algorithmic interpretation of the SQS algorithm. Additionally, Appendix C contains EM examples and implementations of the SQS algorithm with explicit quantum circuits.

Complexity— In the worst case of a maximally entangled state, an EM has n rows, each having one qubit. Each row requires a maximum of two oracle calls, contributing to an overall complexity of $\mathcal{O}(n)$. Thus, optimising the EM to have minimum rows (maximum inter-separable qubits) and minimising the total number of qubits is beneficial. It is possible to map an arbitrary dataset to n qubits such that the $n - 1$ qubits are inter-separable and are only entangled to the last qubit n , thus having only two rows in the EM. This allows one to search for an item in a dataset \mathcal{D} of any size in a maximum of four oracle calls. The only restriction imposed on \mathcal{D} is the knowledge of how to encode and prepare it on a quantum computer. In Appendix A, we present a novel method to encode a dataset \mathcal{D} for an efficient EM. The algorithm itself does not prepare \mathcal{D} or need direct access to \mathcal{D} . If the preparation method for \mathcal{D} has been given by a third

party, the algorithm can search for an entry in \mathcal{D} without accessing the entire dataset. It should be noted that the SQS algorithm requires an ancilla qubit for each data qubit, making a total of $2n$ qubits.

Experimental validation—Working with the quantum computer IBM Kyiv [24–27] for binary datasets of size $N \in \{2^8, 2^{16}, 2^{24}, 2^{32}, 2^{40}\}$ (equal superposition states) yielded the searched bit string. The plots of experimental results for datasets $N \in \{2^8, 2^{16}\}$ are shown in Fig. 3. It shows the search results for the bit strings ‘01010101’ (‘01’ \times 4) and ‘0101010101010101’ (‘01’ \times 8), resulting in 1939 and 735 counts, respectively, in 4096 shots. Here, we obtain low result counts and multiple states due to hardware noise; these can be improved with better hardware optimisation for the proposed algorithm. The experimental runtimes for 4096 shots for $N \in \{2^8, 2^{16}, 2^{24}, 2^{32}, 2^{40}\}$ were $\{9s, 15s, 17s, 34s, 35s\}$, respectively. We experimentally searched an unsorted binary dataset of size over 5TB (40bits \times 2^{40}) in 4096 shots in 35 seconds, resulting in the searched bit string count of four. The experiments’ relevant quantum circuits and plots are available in Appendix C and D. These runtimes may vary with the quantum hardware chosen for computation. The theoretical complexity of the proposed search algorithm is $\mathcal{O}(1)$. Thus, a fully optimised hardware with $2n$ compute nodes working in parallel should have the same run time independent of n , $n = \log_2 N$. The inconsistency in search time and low search count are due to hardware limitations.

Discussion—In conclusion, we have proposed an algorithm that can search for an item in an unsorted dataset faster than the presently known classical or quantum

search algorithm. We show that the search speed of the proposed algorithm depends on the EM. This gives an overwhelming advantage, as it can exhibit an incredibly fast search operation independent of the dataset size N . It is important to note that while the EM organizes the search process, the algorithm’s speed and efficiency fundamentally arise from dividing the search into the subspaces of the qubits. This methodological advantage, guided by the EM, is the key to surpassing the resource requirements of both classical and previous quantum search algorithms.

In the worst possible entanglement structure of maximally entangled n qubits, the proposed quantum algorithm has the complexity of $\mathcal{O}(n)$. However, a dataset can be adeptly mapped into an efficient structure to optimise the EM, allowing the search for any element in a maximum of four oracle calls $\mathcal{O}(1)$. This beats the best quantum search algorithm, Grover’s search $\mathcal{O}(\sqrt{N})$ and the best classical ordered search algorithm, binary search $\mathcal{O}(\log N)$, which requires sorting of the dataset. We have experimentally demonstrated the advantage of the SQS algorithm by searching an unsorted binary dataset of size 5TB 4096 times in 35 seconds on current-generation quantum hardware.

We suggest that a scalable simulation of the proposed algorithm through classical means is possible due to an exponential reduction in the compute node requirements. We refer the reader to Appendix F for a detailed hypothesis. We look forward to a comparative study of the SQS algorithm’s performance against the existing classical search methods.

Acknowledgments—The authors thank IISER Bhopal and IBM Quantum for providing the computational resources to conduct this research. Special thanks to Prabhat Kumar Dubey for his insightful feedback and invaluable assistance in reviewing and rephrasing this manuscript.

Appendix A: Dataset encoding

All classical data numbers, text, or structured records can be losslessly converted to binary strings using standard algorithms [28]. This binary representation enables basis encoding into quantum states, as described in [2]. The process of mapping a dataset \mathcal{D} of size N to quantum states involves assigning each data item a unique binary string of length $n = \lceil \log_2 N \rceil$ and preparing the quantum state via basis encoding.

Encoding a dataset of 2^n entries into $|\psi\rangle$ as 2^n states using n qubits can be done through the operation

$$|\psi\rangle = H^{\otimes n} |0^{\otimes n}\rangle. \quad (\text{A1})$$

This creates an equal superposition of all 2^n states where all n qubits are separable. Here, we shall only have one row in EM, and an entry in the said dataset can be searched in two oracle calls.

Entanglement generation is necessary for a dataset of size between 2^n and 2^{2^n-1} . We propose to map such a dataset using classical methods/algorithms (binary/basis encoding [2, 15, 16]) such that $n - 1$ qubits remain separable and in uniform superposition, and only a single qubit is entangled to every other qubit. The encoding step is performed once per dataset and has complexity $\mathcal{O}(N)$. The unitaries to achieve this are

$$\text{MCX}_n = \begin{bmatrix} \text{I} & 0 & \cdots & 0 & 0 \\ 0 & \text{I} & \cdots & 0 & 0 \\ \vdots & \vdots & \ddots & \vdots & \vdots \\ 0 & 0 & \cdots & \text{I} & 0 \\ 0 & 0 & \cdots & 0 & \text{X} \end{bmatrix},$$

$$\text{MCZ}_n = \begin{bmatrix} \text{I} & 0 & \cdots & 0 & 0 \\ 0 & \text{I} & \cdots & 0 & 0 \\ \vdots & \vdots & \ddots & \vdots & \vdots \\ 0 & 0 & \cdots & \text{I} & 0 \\ 0 & 0 & \cdots & 0 & \text{Z} \end{bmatrix},$$

$$\text{MCH}_n = \begin{bmatrix} \text{I} & 0 & \cdots & 0 & 0 \\ 0 & \text{I} & \cdots & 0 & 0 \\ \vdots & \vdots & \ddots & \vdots & \vdots \\ 0 & 0 & \cdots & \text{I} & 0 \\ 0 & 0 & \cdots & 0 & \text{H} \end{bmatrix}.$$

Here, the Identity Gate I:

$$\text{I} = \begin{pmatrix} 1 & 0 \\ 0 & 1 \end{pmatrix},$$

Pauli-X Gate X:

$$\text{X} = \begin{pmatrix} 0 & 1 \\ 1 & 0 \end{pmatrix},$$

Pauli-Z Gate Z:

$$\text{Z} = \begin{pmatrix} 1 & 0 \\ 0 & -1 \end{pmatrix},$$

Hadamard Gate H:

$$\text{H} = \frac{1}{\sqrt{2}} \begin{pmatrix} 1 & 1 \\ 1 & -1 \end{pmatrix},$$

Rotation Y Gate $\hat{R}_Y(\theta)$ for an arbitrary $\theta \in [0, 2\pi]$:

$$\hat{R}_Y(\theta) = \begin{pmatrix} \cos(\frac{\theta}{2}) & -\sin(\frac{\theta}{2}) \\ \sin(\frac{\theta}{2}) & \cos(\frac{\theta}{2}) \end{pmatrix}. \quad (\text{A2})$$

$\text{MCX}_n, \text{MCZ}_n$ and MCH_n are multi-controlled unitary operations acting on n qubits. The three mentioned control gates act as identity gates for all the qubits except the last. These gates allow the first $n - 1$ qubits to maintain their initial equal superposition states; thus, they can all be searched in parallel. Algorithm (1) provides the pseudocode for such a encoding method.

Algorithm 1 Dataset preparation for an optimal EM

1: Use classical means to map N items to quantum state $|\psi\rangle$ as.

$$|\psi_{\mathcal{D}}\rangle = \sum_{j=1}^N c_j |\psi_j\rangle$$

2: Create an equal superposition state $|\psi_E\rangle$ of all n qubits by $H^{\otimes n}$ operation.

$$|\psi_E\rangle = H^{\otimes n} |0\rangle^{\otimes n}$$

3: **for** all states $|\psi_r\rangle$ in $|\psi_{\mathcal{D}}\rangle$, $|\psi_R\rangle = |\psi_E\rangle - |\psi_{\mathcal{D}}\rangle$ **do**
4: $\triangleright |\psi_R\rangle = \sum c_r |\psi_r\rangle$

5: **procedure** REMOVE STATE $|\psi_r\rangle$

6: define subspace of $|\psi_r\rangle$ for m^{th} qubit as $|\psi_{r_m}\rangle$

$$|\psi_r\rangle = \bigotimes_{m=1}^n |\psi_{r_m}\rangle$$

7: **for** $m = 1$ to $m = n - 1$ **do**

8: **if** $|\psi_{r_m}\rangle = |0\rangle$ **then**

9: Apply X gate on qubit m .

10: **end if**

11: **end for**

12: **if** $|\psi_{r_n}\rangle = |1\rangle$ **then**

13: Apply MCH_n gate on n qubits.

14: **else**

15: Apply $\text{MCZ}_n \cdot \text{MCH}_n$ gate on n qubits.

16: \triangleright First $n - 1$ qubits are control qubits and the n^{th} qubit is the target qubit.

17: **end if**

18: **for** $m = 1$ to $m = n - 1$ **do**

19: **if** $|\psi_{r_m}\rangle = |0\rangle$ **then**

20: Apply X gate on qubit m .

21: **end if**

22: **end for**

23: **end procedure**

24: \triangleright This procedure entangles the last qubit with the rest.

25: **end for**

We only have two rows in the EM, with the first row having $n - 1$ qubits and the second row having the n^{th} qubit. After fixing $n - 1$ qubits in Q_1 in their solution states $|\mathcal{S}_{Q_1}\rangle$ (a total of two oracle calls), we prepare the n^{th} qubit in its respective state and search it (two more oracle calls). This dataset mapping allows searching a dataset of any size or form in a maximum of four oracle calls. A drawback of the algorithm (1) is that both the quantum states containing $|0\rangle$ and $|1\rangle$ cannot be removed together. For example, removing both $|111\rangle$ and $|110\rangle$ is not possible, as it would lead to no measurement on the third qubit. Thus, the entries representing these states have to be mapped to other states that can be removed.

All classical data can be represented as binary strings using standard encoding schemes, such as ASCII for text or IEEE 754 for floating-point numbers. For a comprehensive treatment, we refer the readers to [28]. Any classical dataset \mathcal{D} of size N can be mapped to a set of binary strings of length $n = \lceil \log_2 N \rceil$, and thus to n qubits via basis encoding. This process is standard in both classical and quantum computation [2, 28].

In the encoding method, we must go through all N elements in the data set. Thus, mapping classical-to-quantum states and finding the preparation method for the subsequent quantum states is a one-time preprocessing step with complexity $\mathcal{O}(N)$. Once encoded, the quantum search operates using the preparation method. This one time cost is lower than the fastest known sorting algorithm, quicksort, with complexity $\mathcal{O}(N \log N)$ [13, 14, 28]. Thus with the encoding complexity of $\mathcal{O}(N)$ and the search complexity of $\mathcal{O}(1)$, the SQS algorithm has the potential to transform how we currently handle large databases.

An example for dataset encoding

Consider a dataset \mathcal{D} with four elements. We map them to states ($|00\rangle, |10\rangle, |01\rangle, |11\rangle$). Now we wish to add an element to the dataset; we map it to state $|001\rangle$, then the dataset is remapped using three qubits as ($|000\rangle, |100\rangle, |010\rangle, |110\rangle, |001\rangle$) and contains $2^2 + 1$ elements. We would map the next element to the state $|101\rangle$, and so on. We generate \mathcal{D} on a quantum computer by using the combinations of the operators I, X and MCX_3 gates with an approach similar to algorithm 1. To add the state $|001\rangle$, generate the first two qubits in equal superposition using $H \otimes H \otimes I$ operation, then apply $(X \otimes X \otimes I) \cdot \text{MCX}_3 \cdot (X \otimes X \otimes I)$. More entries can be added to the dataset in a similar manner.

MCH_n gate can be used to pop (remove) an element from a dataset. For example, for a dataset of size 8 (2^3) ($|000\rangle, |100\rangle, |010\rangle, |110\rangle, |001\rangle, |101\rangle, |011\rangle, |111\rangle$). We have created all the states in equal superposition using $H^{\otimes 3}$, and now we wish to remove the element $|101\rangle$. This can be achieved by the operation $(I \otimes X \otimes I) \cdot \text{MCH}_3 \cdot (I \otimes X \otimes I)$, a circuit example is given in Fig. 4. In the circuit, the states are removed by converting them

to another state using the operations between the dotted lines. These operations are commute. Therefore, it is possible to prepare a dataset of any size using only (I, X, H, MCX_n and MCH_n) gates. If structured efficiently (EM with only two rows), any item in the dataset can be searched in a maximum of four oracle calls independent of the number of items N in the dataset.

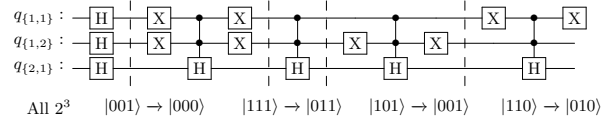


FIG. 4. Example quantum circuit to remove the states from equal superposition of all states. Row 1 has qubits Q_1 , namely $\{q_{\{1,1\}}, q_{\{1,2\}}\}$, which are inter-separable as all control operations are equivalent to I. Row 2 has only $q_{\{2,1\}}$. Here, the arrow represents the probability conversion of one state to another. These operations can be reversed by using controlled $Z \cdot H$ operations instead of the controlled H gate, where Z is the Pauli Z gate. These operations only entangle one qubit with the rest and can be searched in a maximum of four oracle calls. Thus, any dataset with a size varying between 2^n and 2^{n-1} can be created and searched in four oracle calls by extrapolating the quantum circuits shown later in Figs. 14 and 16.

Appendix B: Calculations

1. Building oracle for each subspace

The oracle [29] is defined as a function that marks the correct solution(s) by flipping their phase. Mathematically, the oracle \hat{O} is represented as a unitary operator

$$\hat{O}|\psi\rangle = \begin{cases} -|\psi\rangle, & \text{if } |\psi\rangle = |S\rangle \\ |\psi\rangle, & \text{if } |\psi\rangle = |R\rangle. \end{cases} \quad (\text{B1})$$

The algorithm requires an oracle \hat{O} to be broken down into \hat{O}_m . \hat{O}_m is an operator acting on the subspace of each data qubit q_m and ancilla qubit a_m . It flips the phase of the ancilla qubit a_m for a subspace solution state $|S_m\rangle$ as

$$\hat{O}_m = I \otimes |R_m\rangle \langle R_m| + Z \otimes |S_m\rangle \langle S_m|, \quad (\text{B2})$$

where $|S_m\rangle, |R_m\rangle$ are the solution and non-solution states for the subspace of qubit q_m . For example, for a binary search entry '0101', the solution state $|S\rangle = |0101\rangle$ and $|S_0\rangle = |0\rangle, |R_0\rangle = |1\rangle$. The action of \hat{O}_m can be given as

$$\hat{O}_m |\phi_m\rangle |\psi_m\rangle = \begin{cases} |\phi_m\rangle |\psi_m\rangle, & \text{if } |\phi_m\rangle |\psi_m\rangle = |0_{a_m}\rangle |S_m\rangle \\ |\phi_m\rangle |\psi_m\rangle, & \text{if } |\phi_m\rangle |\psi_m\rangle = |0_{a_m}\rangle |S_m\rangle \\ -|\phi_m\rangle |\psi_m\rangle, & \text{if } |\phi_m\rangle |\psi_m\rangle = |1_{a_m}\rangle |S_m\rangle \\ |\phi_m\rangle |\psi_m\rangle, & \text{if } |\phi_m\rangle |\psi_m\rangle = |1_{a_m}\rangle |R_m\rangle, \end{cases} \quad (\text{B3})$$

where $|\phi_m\rangle$ is the state of the ancilla qubit a_m in binary basis $\{0_{a_m}, 1_{a_m}\}$ and $|S_m\rangle, |R_m\rangle$ are solution and non-solution states for the subspace of qubit q_m . A quantum circuit for an oracle searching for the state $|101\rangle$ in three qubits is given in Fig. B1. The full oracle \hat{O} :

$$\hat{O} = \bigotimes_{m=0}^{n-1} \hat{O}_m \quad (\text{B4})$$

and the circuits for the subspace oracle \hat{O}_m are distinctly marked in the figure as O_m , $m \in \{0, 1, 2\}$.

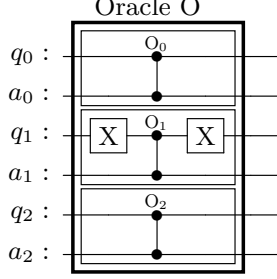


FIG. 5. Representation of an example oracle circuit that marks the state $|101\rangle$. O_m , $m \in \{0, 1, 2\}$ are the oracle circuits for the subspace of qubit q_m . The circuit above would separately mark the subspace solution state of each qubit by flipping the phase of its respective ancilla qubit. For example, an ancilla qubit a_0 will have a phase flip if q_0 is in the state $|1\rangle$ by the action of O_0 . This whole circuit for the operation \hat{O} can be treated as a black box which marks the state $|101\rangle$.

Any bit string can be broken down into individual bits corresponding to the subspace of each qubit. Thus, this transformation of the oracle is possible for all bit strings. It has to be noted that mathematically this oracle function is similar to Grover's oracle, except we have a $2n \rightarrow 2n$ mapping instead of $n \rightarrow n$. The oracle \hat{O} marks a state by flipping the phase of the respective ancilla qubits instead of flipping the state itself. How it's done can be hidden in a black box. If someone provides us with a black box that marks the solution state in the manner described above, we can use the SQS algorithm to find the searched entry with complexity $\mathcal{O}(1)$.

2. Searching all separable qubits

$\hat{F}_m(\theta_m)$ is a two-qubit operator and does not affect other qubits. The general quantum circuit of $\hat{F}_m(\theta_m)$ is given in Fig. 6. Here, $P(\theta_m)$ and $F_m(\theta_m)$ are the quantum circuits for the preparation and fixed point operator defined in Eq. (4 and 11) respectively.

For n qubits in a separable state $|\Psi\rangle$ as

$$|\Psi\rangle = \bigotimes_{m=0}^{n-1} |\Psi_m\rangle = \bigotimes_{m=0}^{n-1} |\psi_m\rangle |0_{a_m}\rangle, \quad (\text{B5})$$

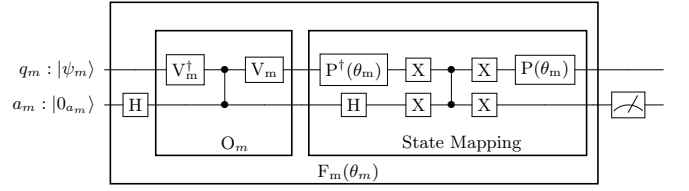


FIG. 6. Quantum circuit representing an iteration of the fixed-point search. V_m is the gate for the basis operation for $|S_m\rangle$ and $|R_m\rangle$. O_m is the subspace oracle circuit of the qubit q_m , it marks the state $|S_m\rangle$ by flipping the phase of ancilla a_m . $P(\theta_m)$ is the state preparation circuit of q_m . We measure a_m after application of the $F_m(\theta_m)$ circuit; if $|1\rangle$ is measured, we have converged to the state $|S_m\rangle$; if $|0\rangle$ is measured, we obtain the state $(\cos(2\theta_m)|R_m\rangle + \sin(2\theta_m)|S_m\rangle)$ and require one more iteration of $F_m(\theta_m)$ for convergence.

where, $|\Psi_m\rangle$ is

$$|\Psi_m\rangle = \begin{bmatrix} \cos \theta_m \\ \sin \theta_m \\ 0 \\ 0 \end{bmatrix}, \quad (\text{B6})$$

defined in the orthogonal basis

$$\{|0_{a_m}\rangle |R_m\rangle, |0_{a_m}\rangle |S_m\rangle, |1_{a_m}\rangle |R_m\rangle, |1_{a_m}\rangle |S_m\rangle\}. \quad (\text{B7})$$

The operator \hat{F} is defined as the combination of operators $\hat{F}_m(\theta_m)$ as

$$\hat{F} = \bigotimes_{m=0}^{n-1} \hat{F}_m(\theta_m), \quad (\text{B8})$$

where $\hat{F}_m(\theta_m)$ is

$$\hat{F}_m(\theta_m) = \begin{bmatrix} -\cos(2\theta_m) & 0 & 0 & -\sin(2\theta_m) \\ -\sin(2\theta_m) & 0 & 0 & \cos(2\theta_m) \\ 0 & 0 & 1 & 0 \\ 0 & 1 & 0 & 0 \end{bmatrix}, \quad (\text{B9})$$

where, $\hat{F}_m(\theta_m)$ marks the ancilla qubit a_m by changing its state from $|0\rangle$ to $|1\rangle$ if the qubit q_m is in the state $|S_m\rangle$. The action of $\hat{F}_m(\theta_m)$ on $|\Psi_m\rangle$ is

$$\hat{F}_m(\theta_m) |\Psi_m\rangle = \begin{bmatrix} -\cos \theta_m \cos 2\theta_m \\ -\cos \theta_m \sin 2\theta_m \\ 0 \\ \sin \theta_m \end{bmatrix}. \quad (\text{B10})$$

Thus the action of the operator \hat{F} on the state $|\Psi\rangle$ is given as

$$\hat{F} |\Psi\rangle = \bigotimes_{m=0}^{n-1} \hat{F}_m(\theta_m) |\Psi_m\rangle. \quad (\text{B11})$$

Here, we show the operator \hat{F} can be applied to any number of separable qubits n at once. This allows us to search multiple separable qubits with a quantum circuit of constant depth, which is twice the depth of the circuit shown in the Fig 6.

3. Searching entangled qubits

The algorithm (2) represents the SQS algorithm in algorithmic format which can search through entangled qubits using EM.

Algorithm 2 Structured Quantum Search

```

1: Generate EM with the dataset preparation method.
2: for each row  $r$  in EM do
3:   for qubit at index  $c \in \{1, \dots, n_r\}$  do
4:     procedure PREPARATION OF QUBIT  $q_{\{r,c\}}$ 
5:       if  $r = 1$  then
6:         Apply  $\hat{F}(\gamma_{\{1,c\}})$  to prepare  $q_{\{1,c\}}$  in  $|\phi_{\{1,c\}}\rangle$ .
7:       else
8:         Apply  $\hat{M}_{\{r,c\}}$  to prepare  $q_{\{r,c\}}$  in  $|\phi_{\{r,c\}}\rangle$ .
9:          $\triangleright$  Created states containing  $|\mathcal{S}_{\mathcal{Q}_{r-1}}\rangle$ .
10:      end if
11:    end procedure
12:    procedure FIXED POINT QUANTUM SEARCH
13:      Apply  $\hat{F}(\gamma_{\{r,c\}})$  on  $q_{\{r,c\}}$  and  $a_{\{r,c\}}$ .
14:      Measure the ancilla qubit  $a_{\{r,c\}}$ .
15:      if ( $a_{\{r,c\}}$  is in state  $|0\rangle$ ) then
16:        Apply  $\hat{F}(\gamma_{\{r,c\}})$  on  $q_{\{r,c\}}$  and  $a_{\{r,c\}}$ .
17:        Measure the ancilla qubit  $a_{\{r,c\}}$ .
18:      end if  $\triangleright$  Applied  $\hat{F}(\gamma_{\{r,c\}})$  twice.
19:    end procedure
20:    if ( $a_{\{r,c\}}$  is in state  $|0\rangle$ ) then
21:      Solution is not present. Terminate Search.
22:     $\triangleright$  A qubit failed to converge, search failed.
23:    else  $\triangleright$  Searched qubit converged to  $S_{\{r,c\}}$ .
24:    end if
25:  end for  $\triangleright$  Qubits in  $Q_r$  are searched in parallel.
26:  All  $Q_r$  are in their solution states  $S_{Q_r}$ .
27:   $\triangleright$  Continue to search the next row.
28: end for
29: if (All measured ancilla  $a_{\{r,c\}}$  are in  $|1\rangle$ ) then
30:   $\triangleright$  All data qubits converged to solution states.
31:  Search complete; the solution state  $|S\rangle$  is found.
32: end if

```

A quantum circuit to prepare and search a qubit $q_{\{r,c\}}$ is given by Fig. 7. $B_{\mathcal{Q}_{r-1}}$ is the basis operator that converts an arbitrary basis to $|\mathcal{S}_{\mathcal{Q}_{r-1}}\rangle$ and $|\mathcal{R}_{\mathcal{Q}_{r-1}}\rangle$ basis. $B_{\mathcal{Q}_{r-1}}$ is used to create the quantum circuit $M_{\{r,c\}}$. The circuit block $M_{\{r,c\}}$ represents the preparation method operator given in Eq. (24). The circuit block $F(\gamma_{\{r,c\}})$ is equivalent to the fixed point operator defined in Eq. (10). We use this $F(\gamma_{\{r,c\}})$ circuit to search for the solution state $|S_{\{r,c\}}\rangle$ in qubit $q_{\{r,c\}}$. In the control operations the qubit $q_{\{r,c\}}$ is taken as the target qubit and \mathcal{Q}_{r-1} qubits as the control qubits.

Appendix C: Examples

Figure 8 shows a Qiskit circuit that searches the state $|0101\rangle$ in stating states of 2^4 separable states in equal superposition. Here $q_0 - q_3$ are the data qubits, and $\text{anc}_0 - \text{anc}_3$ are their respective ancilla qubits. Addition-

ally, c and cqq represent the classical register to store measurements of data and ancilla qubits, respectively. The state_prep circuit block and its adjoint state_prep_dg circuit block represent $H^{\otimes 4}$ gates acting on the four data qubits. All the other quantum gates used have their usual meaning. This circuit can be extrapolated using more qubits to search within an exponentially larger number of separable states in equal superposition.

1. EM examples

EM is essentially the relabeling of qubits to represent their entanglement order. It contains multiple rows, where each row has a set of qubits that are inter-separable. EM is constituted in a way that the first row contains independent qubits, whereas the second-row qubits depend on the first row, the third on the first two rows, and so on. Note that the first row would also contain the qubits that act as control qubits in the controlled operations. An EM of n separable qubits only has one row containing all the qubits, as

$$\text{EM} = \left| \left| q_{\{1,1\}} \ q_{\{1,2\}} \ \dots \ q_{\{1,n\}} \right| \right|, \quad (\text{C1})$$

its quantum circuit is shown in Fig. 9.

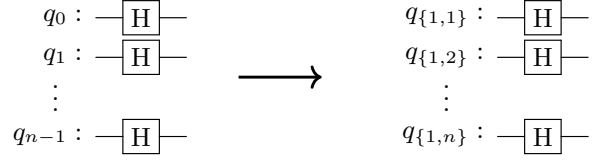


FIG. 9. The circuit on the left shows the preparation operator representation of n separable qubits, and the right shows its EM representation.

An EM of n qubits where $n - 1$ are inter-separable and are only entangled to the last qubit n has two rows. The first row has qubits Q_1 which contains the $n - 1$ inter-separable qubits, and the second row has Q_2 containing the last qubit q_{n-1} . We write the EM as

$$\text{EM} = \left| \left| \begin{array}{c} q_{\{1,1\}} \ q_{\{1,2\}} \ \dots \ q_{\{1,n-1\}} \\ q_{\{2,1\}} \end{array} \right| \right|, \quad (\text{C2})$$

and its associated circuit is shown in Fig. 10.

A maximally entangled state of n qubits shall have n rows in EM, each containing a single qubit. Here we write the EM as

$$\text{EM} = \left| \left| \begin{array}{c} q_{\{1,1\}} \\ q_{\{2,1\}} \\ \vdots \\ q_{\{n,1\}} \end{array} \right| \right|, \quad (\text{C3})$$

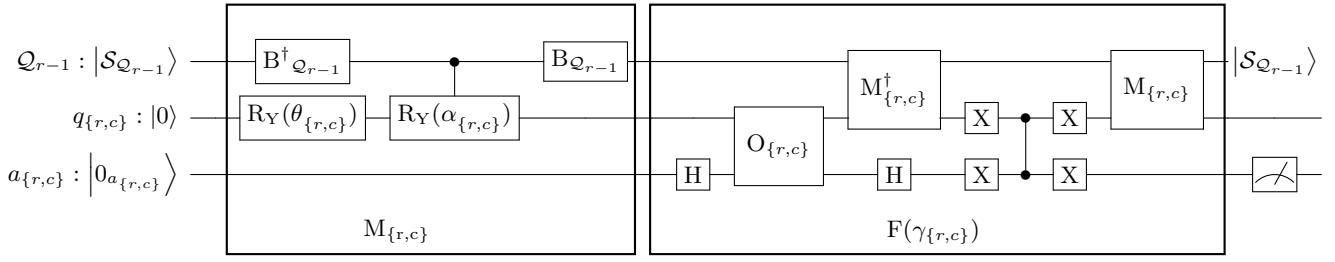


FIG. 7. An iteration of fixed-point search for the entangled qubit $q_{\{r,c\}}$ at row r and index c in the EM. $B_{Q_{r-1}}$ is the circuit for the basis operator that changes the current basis to $|\mathcal{S}_{Q_{r-1}}\rangle$ and $|\mathcal{R}_{Q_{r-1}}\rangle$ basis. The quantum circuit $M_{\{r,c\}}$ represents the circuit for the state preparation operation defined in Eq. (24). $O_{\{r,c\}}$ represents the oracle circuit for the subspace of qubit $q_{\{r,c\}}$ flipping the phase of $a_{\{r,c\}}$ for qubit $q_{\{r,c\}}$ in the state $|S_{\{r,c\}}\rangle$. The whole circuit shown above is applied to search for the state $|S_{\{r,c\}}\rangle$ in $q_{\{r,c\}}$ after converging all Q_{r-1} qubits to state $|\mathcal{S}_{Q_{r-1}}\rangle$.

its circuit is shown by Fig. 11.

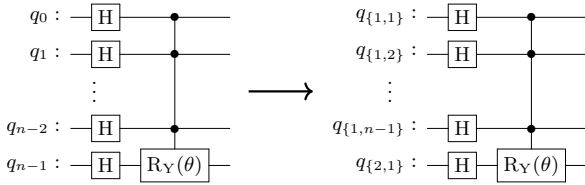


FIG. 10. The circuit on the left shows the preparation operator representation of $n - 1$ inter-separable qubits entangled with the last qubit, and the circuit on the right shows its EM representation.

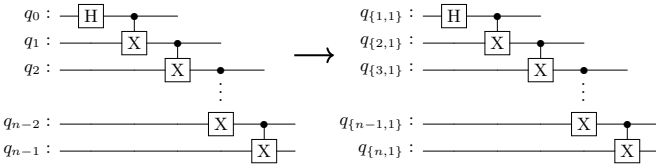


FIG. 11. The circuit on the left shows the preparation operator representation of n maximally entangled qubits, and the circuit on the right shows its EM representation.

Similarly, Fig. 12 shows an arbitrary quantum circuit. We observe that qubits q_1 and q_3 act only as control qubits and thus are inter-separable and placed in the first row. The qubits, q_0 , q_2 and q_4 are entangled and depend on the state of the first row qubits q_1 and q_3 . These are thus placed in the second row. Similarly, the qubit q_5 depends on qubit q_3 and q_4 and is placed in the third row. Thus the EM is

$$\text{EM} = \left\| \begin{array}{ccc} q_{\{1,1\}} & q_{\{1,2\}} & \\ q_{\{2,1\}} & q_{\{2,2\}} & q_{\{2,3\}} \\ q_{\{3,1\}} & & \end{array} \right\|. \quad (\text{C4})$$

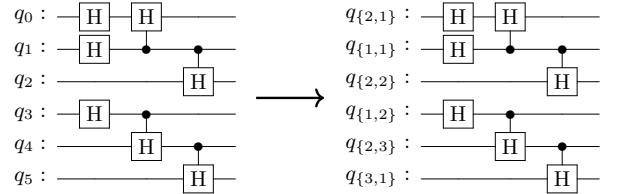


FIG. 12. On the left show, we have an arbitrary preparation operator circuit, and the circuit on the right shows its EM representation. Here, the qubits q_1 and q_3 act only as control qubits and thus are inter-separable and placed in the first row. The qubits, q_0 , q_2 and q_4 are entangled and depend on the state of the first row qubits q_1 and q_3 . These are thus placed in the second row. Similarly, the qubit q_5 depends on qubit q_3 and q_4 thus is placed in the third row.

2. Search example on four qubit dataset

Let us take an example dataset of four qubits for better understanding. We start with a dataset \mathcal{D} containing all possible 2^4 states for

$$\mathcal{D} = \{0000, 0001, 0010, 0011, 0100, 0101, 0110, 0111, 1000, 1001, 1010, 1011, 1100, 1101, 1110, 1111\}. \quad (\text{C5})$$

We would search the bit string ‘1010’ for demonstration. Four separable qubits $q_{\{1,1\}} - q_{\{1,4\}}$ can be searched simultaneously using the operator $\hat{F}_{\{1,i\}}(\frac{\pi}{4})$, $i \in \{1, 2, 3, 4\}$. The EM for the four separable qubits has a single row containing all the qubits as

$$\text{EM} = \left\| q_{\{1,1\}} \quad q_{\{1,2\}} \quad q_{\{1,3\}} \quad q_{\{1,4\}} \right\|, \quad (\text{C6})$$

The quantum circuit for the operator $\hat{F}_{\{1,i\}}(\frac{\pi}{4})$ is given by Fig. 13.

The state preparation is the equal superposition of all possible states of four qubits. This is achieved by

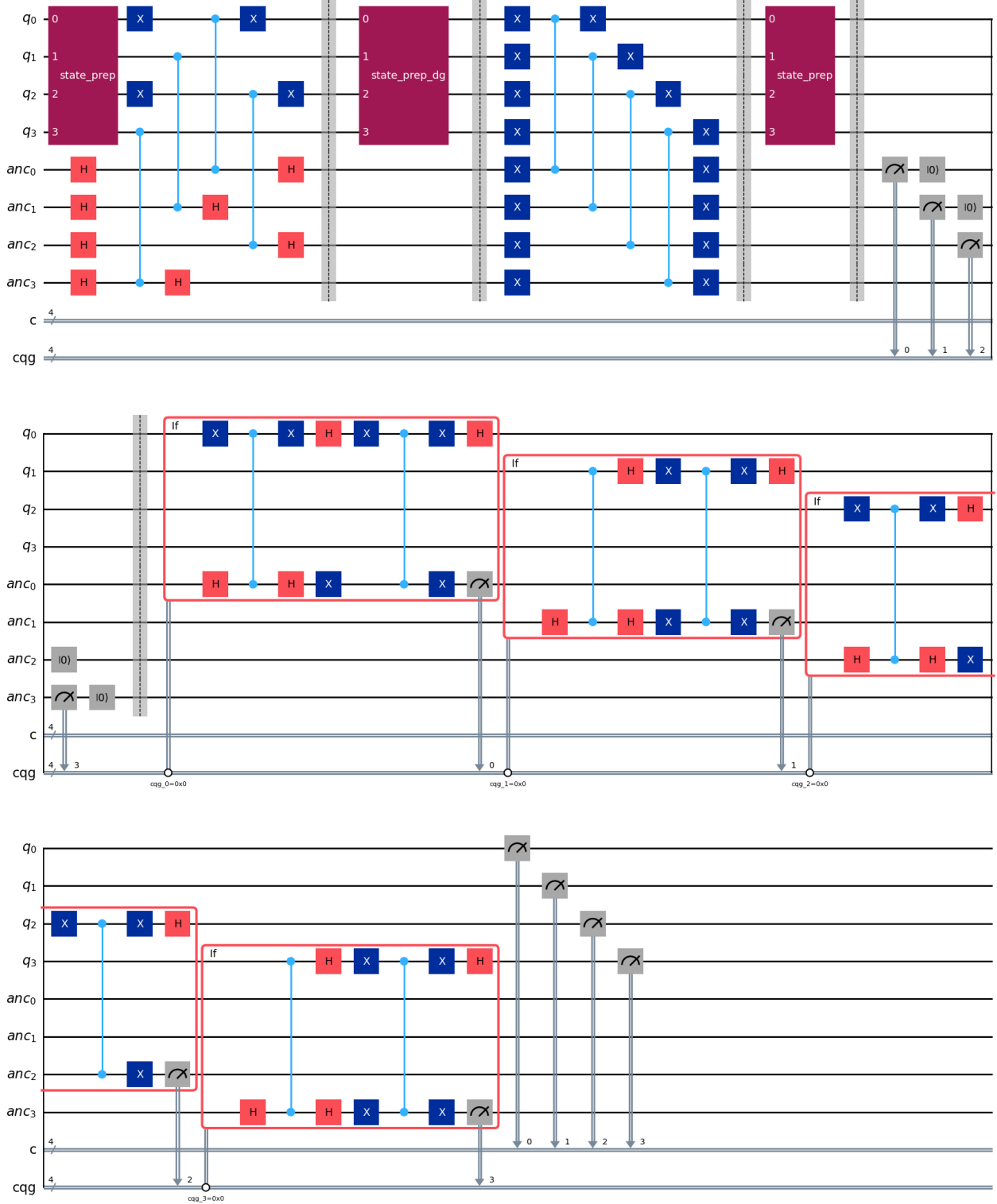


FIG. 8. Example Qiskit[30],[31] circuit representation for search on an equal superposition of four qubits (state_prep is $H^{\otimes 4}$). Here $q_0 - q_3$ are the data qubits, and $anc_0 - anc_3$ are their respective ancilla qubits. Additionally, c and cqg represent the classical register to store measurements of data and ancilla qubits, respectively. The state_prep circuit block and its adjoint state_prep_dg circuit block represent $H^{\otimes 4}$ gates acting on the four data qubits. All the other quantum gates used have their usual meaning. Here, the oracle is marking the state $|0101\rangle$ by flipping the phase of ancilla qubits. In this circuit the operation $\hat{F}_m(\frac{\pi}{4})$ is applied twice for convergence to the solution state $|0101\rangle$.

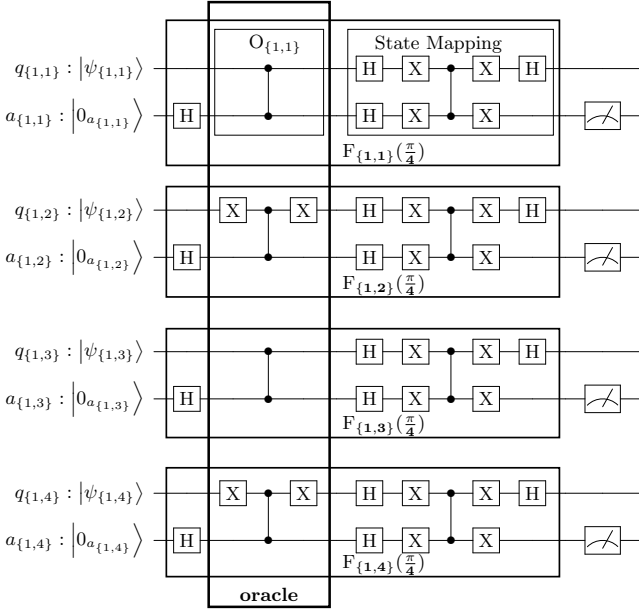


FIG. 13. The quantum circuit $F_{\{1,c\}}(\frac{\pi}{4})$, $c \in \{1, 2, 3, 4\}$ of the fixed-point operators. The circuit $F_{\{1,1\}}(\frac{\pi}{4})$ searches for state $|1\rangle$ in qubit $q_{\{1,1\}}$ with labeled operations. We should achieve our desired result in two calls to this whole circuit. $O_{\{1,1\}}$ is the oracle circuit for the subspace of $q_{\{1,1\}}$ marking the state $|1\rangle$. The whole oracle function searching for the state $|1010\rangle$ has been shown in the figure.

$H^{\otimes 4} |0000\rangle$. The operator:

$$\begin{aligned} \hat{F}_{\{1,1\}}(\frac{\pi}{4}) & \text{ searches for state } |S_{\{1,1\}}\rangle = |0\rangle \text{ in qubit } q_{\{1,1\}}; \\ \hat{F}_{\{1,2\}}(\frac{\pi}{4}) & \text{ searches for state } |S_{\{1,2\}}\rangle = |1\rangle \text{ in qubit } q_{\{1,2\}}; \\ \hat{F}_{\{1,3\}}(\frac{\pi}{4}) & \text{ searches for state } |S_{\{1,3\}}\rangle = |0\rangle \text{ in qubit } q_{\{1,3\}}; \\ \hat{F}_{\{1,4\}}(\frac{\pi}{4}) & \text{ searches for state } |S_{\{1,4\}}\rangle = |1\rangle \text{ in qubit } q_{\{1,4\}}. \end{aligned}$$

We apply these operators in parallel on the preparation state of \mathcal{D} twice to converge to the solution state $|1010\rangle$ in two oracle calls. The circuit for the full search operation is given by Fig. 14.

Now, let us remove the entry ‘1101’ from the dataset. The new dataset \mathcal{D}' looks like

$$\mathcal{D}' = \{0000, 0001, 0010, 0011, 0100, 0101, 0110, 0111, 1000, 1001, 1010, 1011, 1100, 1110, 1111\}. \quad (C7)$$

The native state preparation of this dataset can be achieved by the circuit in Fig. 15 using the methods given in the algorithm (1). Figure 17 shows the simulated probability distribution of \mathcal{D}' .

Here, the EM is:

$$\text{EM} = \left\| \begin{array}{ccc} q_{\{1,1\}} & q_{\{1,2\}} & q_{\{1,3\}} \\ q_{\{2,1\}} & & \end{array} \right\|. \quad (C8)$$

We have 4 entangled qubits in two rows as $\{q_{\{1,1\}}, q_{\{1,2\}}, q_{\{1,3\}}\}$, and $\{q_{\{2,1\}}\}$. Here Q_1 is an array of 3

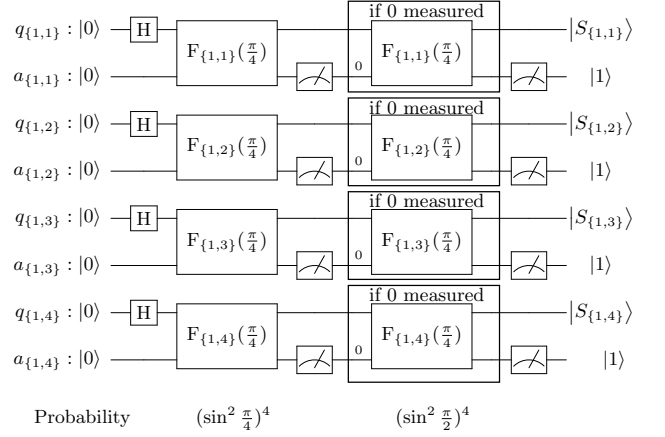


FIG. 14. Quantum circuit for searching in equal superposition states of four qubits. Finally, we have measured all ancilla qubits in the state $|1\rangle$. Thus, the solution is found, and measuring the qubits $q_{\{1,1\}} - q_{\{1,4\}}$ would yield ‘1010’.

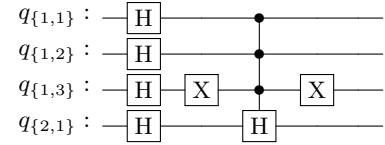


FIG. 15. Quantum circuit for the state preparation of the fifteen states in \mathcal{D}' . Entry ‘1011’ is popped using a multi-controlled Hadamard gate. Here row 1 has qubits Q_1 namely $\{q_{\{1,1\}}, q_{\{1,2\}}, q_{\{1,3\}}\}$, these three are inter-separable as the multi-control operation acts as an identity operator to these states. Row 2 has $q_{\{2,1\}}$ only.

qubits that are inter-separable and can thus be searched simultaneously. The qubit $q_{\{2,1\}}$ can only be searched after all qubits Q_1 have been found in their solution states $|S_{Q_1}\rangle$. The quantum circuit to search for string ‘1010’ is given in Fig. 16. Here, we first searched and locked the qubits $q_{\{1,c\}}$ and then proceeded to prepare and search the $q_{\{2,1\}}$ qubit in the second row. After the final measurement, we have found the solution state if all the ancillas are measured in the state $|1\rangle$. Otherwise, the solution state does not exist in the dataset. The simulated search results for the state $|1010\rangle$ and the state $|1101\rangle$ in dataset \mathcal{D}' are given in Fig. 18. Here, we find the state $|1010\rangle$ with a probability of 1 but fail to find the state $|1101\rangle$ (probability 0) as it does not exist in \mathcal{D}' . This shows that our algorithm can deterministically answer whether the searched entry is present in a dataset or not. Note that for a dataset with EM of this structure (two rows), we can search for any element by adjusting the oracle in the same amount of time, regardless of the dataset size.

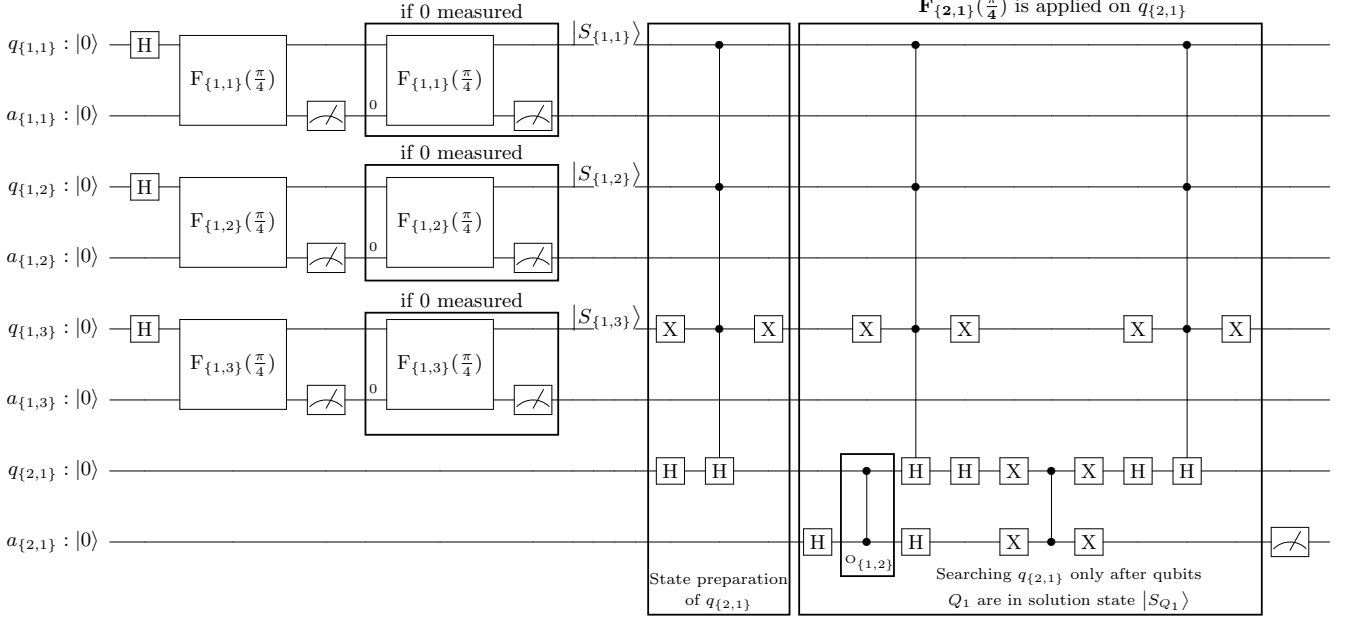


FIG. 16. Searching the above dataset for bit string ‘1010’. First we searched and locked the qubits $q_{\{1,c\}}$ using the circuit blocks $F_{\{1,c\}}(\frac{\pi}{4})$, $c \in \{1, 2, 3\}$. Then we proceeded to prepare and then search the $q_{\{2,1\}}$ qubit in second row with the circuit block $F_{\{2,1\}}(\frac{\pi}{4})$. One more iteration of $F_{\{2,1\}}(\frac{\pi}{4})$ is required to achieve the solution state $|S_{\{2,1\}}\rangle$ for $q_{\{2,1\}}$ with full certainty. After the final measurement, we have found the solution state if all the ancillas are measured in the state $|1\rangle$. Otherwise, the solution state does not exist in the dataset.

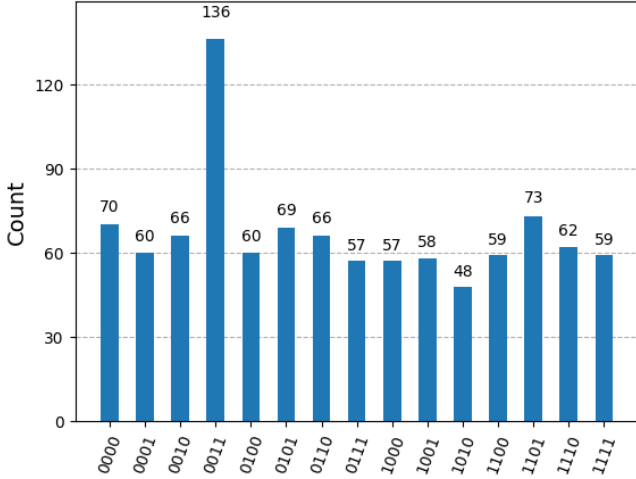
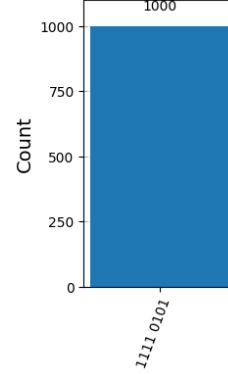
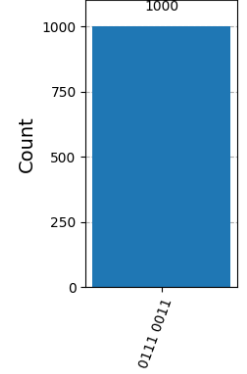


FIG. 17. The probability distribution of \mathcal{D}' with a total measurement counts of ‘1000’. The state $|1101\rangle$ has probability 0, and the state $|1100\rangle$ has twice the probability compared to other states.



(a) State $|1010\rangle$ found.



(b) State $|1101\rangle$ not found.

FIG. 18. The figure (a) demonstrates the state $|1010\rangle$ is found with probability 1 in the dataset \mathcal{D}' . The figure (b) shows the state $|1101\rangle$ is found with probability 0 in \mathcal{D}' . The total number of shots for the simulation was 1000, each requiring four oracle calls. The top four qubits are the data qubits representing the bit string measured, and the bottom four are the respective ancilla qubits. The searched bit string is found if all the ancilla qubits are in the state $|1\rangle$. In (b), the fourth qubit has failed to converge to its solution state, denoted by the last ancilla in state $|0\rangle$.

$n = \log_2 N$, parallel compute nodes, at maximum, only needs to process $(2^2 + n)$ states on a single node, where N is the size of the dataset. The algorithm runs a significant workload in parallel and, in theory, should perform well in an ideal classical simulation. Theoretically, for a data set of size 2^n , $n \in \{1, 2, \dots\}$ running on $2n$ nodes, the runtime is independent of n . The circuit in Fig. 8 reduced to a single data qubit along with its ancilla qubit required an

Nvidia RTX A5000 GPU [32] (total 8192 CUDA cores) $32\mu\text{s}$ to run. The theory allows searching a dataset of more than 2^{1000} on the same hardware optimised to run in parallel compute nodes of the GPU in a similar time requirement. Thus with the encoding complexity of $\mathcal{O}(N)$ and the search complexity of $\mathcal{O}(1)$, the SQS algorithm has the potential to transform how we currently handle large databases.

-
- [1] C. H. Bennett, E. Bernstein, G. Brassard, and U. Vazirani, Strengths and weaknesses of quantum computing, *SIAM Journal on Computing* **26**, 1510 (1997), <https://doi.org/10.1137/S0097539796300933>.
- [2] M. A. Nielsen and I. L. Chuang, *Quantum Computation and Quantum Information* (Cambridge University Press, 2000).
- [3] A. W. Harrow and A. Montanaro, Quantum computational supremacy, *Nature* **549**, 203 (2017).
- [4] L. Gyongyosi and S. Imre, A survey on quantum computing technology, *Comput. Sci. Rev.* **31**, 51 (2019).
- [5] L. K. Grover, A fast quantum mechanical algorithm for database search, in *Proceedings of the Twenty-Eighth Annual ACM Symposium on Theory of Computing* (1996) pp. 212–219.
- [6] M. Boyer, G. Brassard, P. Høyer, and A. Tapp, Tight bounds on quantum searching, *Fortschritte der Physik* **46**, 493–505 (1998).
- [7] G. Brassard, Searching a quantum phone book, *Science* **275**, 627 (1997).
- [8] K. Das and A. Sadhu, Experimental study on the quantum search algorithm over structured datasets using ibmq experience, *Journal of King Saud University - Computer and Information Sciences* **34**, 10.1016/j.jksuci.2022.01.012 (2022).
- [9] T. Hogg, A framework for structured quantum search, *Physica D: Nonlinear Phenomena* **120**, 102–116 (1998).
- [10] Y. He and J. Sun, Quantum search in structured database, in *Advances in Natural Computation*, edited by L. Wang, K. Chen, and Y. S. Ong (Springer Berlin Heidelberg, Berlin, Heidelberg, 2005) pp. 434–443.
- [11] A. M. Childs, A. J. Landahl, and P. A. Parrilo, Quantum algorithms for the ordered search problem via semidefinite programming, *Physical Review A* **75**, 10.1103/physreva.75.032335 (2007).
- [12] E. Bernstein and U. Vazirani, Quantum complexity theory, in *Proceedings of the Twenty-Fifth Annual ACM Symposium on Theory of Computing*, STOC '93 (Association for Computing Machinery, New York, NY, USA, 1993) p. 11–20.
- [13] L. F. Williams, A modification to the half-interval search (binary search) method, in *Proceedings of the 14th Annual ACM Southeast Regional Conference*, ACMSE '76 (Association for Computing Machinery, New York, NY, USA, 1976) p. 95–101.
- [14] A. Shabbir, A. Majeed, M. Iftikhar, R. H. Ali, U. Arshad, M. Z. Shabbir, A. Z. Ijaz, N. Ali, and A. Aftab, A review of algorithms's complexities on different valued sorted and unsorted data, 2023 International Conference on IT and Industrial Technologies (ICIT) , 1 (2023).
- [15] S. Sharma and R. N, Survey of encoding techniques for quantum machine learning, *Cybernetics and Physics* **13**, 152 (2024).
- [16] M. Rath and H. Date, Quantum data encoding: a comparative analysis of classical-to-quantum mapping techniques and their impact on machine learning accuracy, *EPJ Quantum Technology* **11**, 72 (2024).
- [17] T. J. Yoder, G. H. Low, and I. L. Chuang, Fixed-point quantum search with an optimal number of queries, *Physical Review X* **4**, 041013 (2014).
- [18] G. Brassard, P. Høyer, and A. Tapp, Quantum counting, in *Proceedings of the Twenty-Fifth International Colloquium on Automata, Languages and Programming* (1998) pp. 820–831.
- [19] T. J. Yoder, G. H. Low, and I. L. Chuang, Fixed-point quantum search with an optimal number of queries, *Physical Review Letters* **113**, 210501 (2014).
- [20] A. M. Dalzell, T. J. Yoder, and I. L. Chuang, Fixed-point adiabatic quantum search, *Physical Review A* **95**, 012311 (2017).
- [21] L. Li, Revisiting fixed-point quantum search: Proof of the quasi-chebyshev lemma, arXiv preprint arXiv:2403.02057 (2024).
- [22] L. K. Grover, Fixed-point quantum search, *Physical Review Letters* **95**, 150501 (2005).
- [23] A. Mizel, Critically damped quantum search, *Phys. Rev. Lett.* **102**, 150501 (2009).
- [24] Angle dependence of the self-acceptance fraction nb for ibm quantum platforms (a) sherbrooke, (b) kyiv, (c) osaka, (d) brisbane and (e) kyoto (2024).
- [25] I. Q. Documentation, Fakekyiv (latest version) (2025).
- [26] Ibm quantum platform.
- [27] I. Quantum, Quantum hardware (2021), accessed: 2025-02-20.
- [28] S. Oualline, *Advanced Binary for Programming & Computer Science: Logical Bitwise and Arithmetic Operations and Data Encoding and Representation* (Independently published, 2020).
- [29] L. K. Grover, Quantum computers can search rapidly by using almost any transformation, *Phys. Rev. Lett.* **80**, 4329 (1998).
- [30] A. Javadi-Abhari, M. Treinish, K. Krsulich, C. J. Wood, J. Lishman, J. Gacon, S. Martiel, P. Nasion, L. S. Bishop, A. W. Cross, B. R. Johnson, and J. M. Gambetta, Quantum computing with qiskit (2024).
- [31] Qiskit Community, Qiskit: An open-source framework for quantum computing (2017).
- [32] N. Corporation, Nvidia rtx a5000 datasheet (2025), accessed: 2025-04-04.